THE JOURNAL OF PHYSICAL CHEMISTRY C

Article

Cite This: J. Phys. Chem. C 2019, 123, 19862−19870

pubs.acs.org/JPCC

Enhanced Spontaneous Emission Rate in a Low-Q Hybrid Photonic-Plasmonic Nanoresonator

Belkıs Gökbulut,[†] Arda Inanç,[†] Gokhan Topcu,[‡] Seçil S. Unluturk,[§] Serdar Ozcelik,[§] Mustafa M. Demir,[‡] and M. Naci Inci*[,†]

[†]Department of Physics, Bogazici University, Bebek, Istanbul, 34342, Turkey

[‡]Department of Materials Science and Engineering, Izmir Institute of Technology, Urla, 35430 Izmir, Turkey

[§]Department of Chemistry, Izmir Institute of Technology, Urla, 35430 Izmir, Turkey

ABSTRACT: In this paper, CdTe quantum dots (QDs)-doped single electrospun polymer nanofibers are partially coated with gold nanoparticles to form distinct hybrid photonic-plasmonic nanoresonators to investigate the critical role of the cavity-confined hybrid mode on the modification of the spontaneous emission dynamics of the fluorescent emitters in low-Q photonic cavities. A total enhancement factor of 11.2 is measured via a time-resolved experimental technique, which shows that there is an increase of about three times in the spontaneous emission rate for the QDs-doped gold nanoparticle-decorated nanofibers as they are compared with those uncoated ones. The physical mechanism affecting the spontaneous emission rate of the encapsulated QDs in such a hybrid photonic-plasmonic nanoresonator is explained to be due to regeneration of the mode field in the nanofiber cavity upon the interaction of the dipoles with the surface plasmons of distinctive gold nanoparticles that surround the outer surface of the nanofiber.

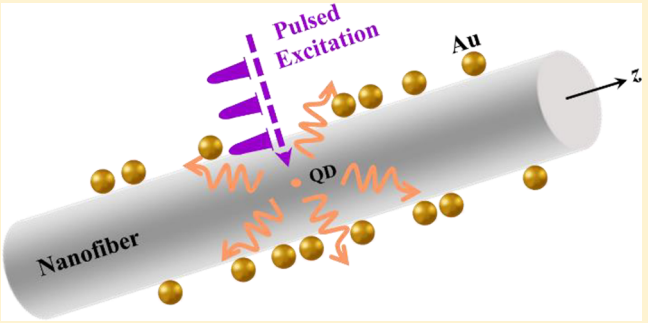

1. INTRODUCTION

Plasmonic nanostructures offer an attractive alternative to dielectric photonic cavities since metallic nanoparticles are extremely capable of confining light within subwavelength volumes and, consequently, enhancing the density of electromagnetic states meaningfully,[1−4] through exciting the collective electrons on the surface of these nanoparticles. Absorption and radiation losses in a metallic cavity are known to cause an exceedingly low Q-factor,[5] nevertheless, confining light waves into a deep subwavelength region of such structure facilitates obtaining an ultrasmall mode volume,[6] which is a crucial design parameter in improving the emission dynamics and optical response of many photonic devices, such as plasmonic nanolasers,[7] nanoantennas,[8] or resonators,[9] etc. On the other hand, hybrid photonic designs in which the dielectric microcavities are covered by metallic layers were demonstrated to have a decreased Q-factor when compared to the bare microcavities.[10,11] Nonetheless, realization and characterization of hybrid cavity systems originating from individual metal nanoparticles in a high Q-factor dielectric photonic structure was demonstrated to unveil the potentially increased interaction between the cavity mode and the quantum emitters.[12,13] For instance, a hybrid photonic crystal cavity with a gold nanorod placed in the center of the crystal was reported to maintain improved cavity characteristics by plasmonic features as a result of the coupling of approximately 40% plasmon-enhanced emission into the cavity mode.[14] Furthermore, a hybrid microcavity with a dipolar plasmonic antenna was analytically modeled to verify a boosted spontaneous emission rate, breaking the fundamental limit on the enhancement rate achieved by a single nanoantenna.[15] A hybrid photonic-plasmonic structure, which is comprised of a metal nanoparticle and a WGM microcavity, was also theoretically revealed to have advantages over a sole microcavity or a sole metal nanoparticle.[16] Light−matter interaction and single-atom cooperativity in such a hybrid structure were demonstrated to enhance considerably since the interrogated metal nanoparticle to the WGM microcavity functioned quite efficiently in confining photon energy, reducing the mode volume, and magnifying the local field.

In this work, CdTe QDs-doped single electrospun polymer nanofibers are partially decorated with separate gold nanoparticles to construct hybrid photonic-plasmonic nanoresonators, which enable surface plasmons to localize in the subwavelength region and give rise to the regeneration of the cavity mode field in each single nanofiber assembly, to enhance the emission rate of the encapsulated QDs to a considerable extent. The proposed photonic design makes a distinctive basis available to explore the crucial role of the hybrid photonic-plasmonic mode field on the modification of the spontaneous emission rate of the quantum emitters in a low-Q photonic structure. As the discrete gold nanoparticles serve as plasmonic

Received: June 3, 2019
Revised: July 11, 2019
Published: July 23, 2019

DOI: 10.1021/acs.jpcc.9b05289
J. Phys. Chem. C 2019, 123, 19862−19870

nanoantennas, which generate intense electromagnetic field regions by extreme light concentrations, each polymer nanofiber provides an ideal platform to confine the fluorescent emission from the excited QDs. The emission dynamics of the encapsulated CdTe QDs, which are coupled to the hybrid modes, is studied via fluorescence decay curves of the emitters using a picosecond time-resolved spectroscopic technique. Although the composite photonic-plasmonic structure proposed here is assumed to be in a low Q-factor regime, a substantially decreased mode volume in the presence of gold nanoparticles proves to strengthen the effective light−matter interaction through dramatically increased local optical field around the quantum emitters. Thus, the spontaneous emission rate of the encapsulated QDs in gold nanoparticle-decorated nanofibers is measured to be enhanced by a factor of 11.2, which is about three times greater than that of the spontaneous decay rate measured in uncoated CdTe QD-doped nanofibers. Such a leaky dielectric hybrid nanoresonator proposed in this work opens a new route to efficiently enhance the emission dynamics of the quantum emitters in photonic structures, which possess low Q-factors.

2. MECHANISM OF THE SPONTANEOUS EMISSION RATE

Modification of the spontaneous decay rate of a quantum emitter, surrounded by a photonic cavity, is described by the Purcell factor, provided that the emitter's transition wavelength is spectrally tuned with the cavity's resonance mode,[17] which is given by

$$F_P = \frac{3Q(\lambda_c/n)^3}{4\pi^2 V} \quad (1)$$

where λ_c is the wavelength of the cavity mode in concern, n is the refractive index of the medium, Q is the quality factor of the optical mode, which is expressed by $Q = \lambda_c/\Delta\lambda_c$ for the high-Q optical cavities, given that the emitter's line width is assumed to be narrower than that of the cavity mode.[18] V is the mode volume, which is determined by integrating the electric field intensity for the cavity mode over a volume and normalizing it to the maximum field intensity.[19] However, the Purcell formula given by eq 1 is based on the assumption that a perfect coupling of the quantum emitter into the resonant cavity mode exists. Additionally, the medium is assumed to be lossless and nondispersive.

In this work, CdTe QD-doped nanofibers are partially coated by gold nanoparticles to construct hybrid photonic-plasmonic nanoresonators to enhance the spontaneous emission rate of the encapsulated QDs. Nanofibers are made of a polymer solution (PVA−PAA) and surrounded by an air cladding, which are considered to be infinitely long compared to their cross-sectional diameters. They are excited by a pulsed laser beam that is incident onto the lateral surface of the nanofibers as illustrated in Figure 1a. Light waves emitted by QDs are coupled into the photonic-plasmonic nanofiber resonator and are guided by the boundary conditions due to Fresnel reflectivity to form standing waves inside the photonic structure. However, since the photonic structure proposed here is assumed to be in a low-Q optical regime, it causes a radiation leakage and the electromagnetic field dissipates away from the photonic resonator. Although light confinement of the excited QDs inside the nanofiber results in the enhanced spontaneous emission rate, conversely, the leaky nature of the hybrid

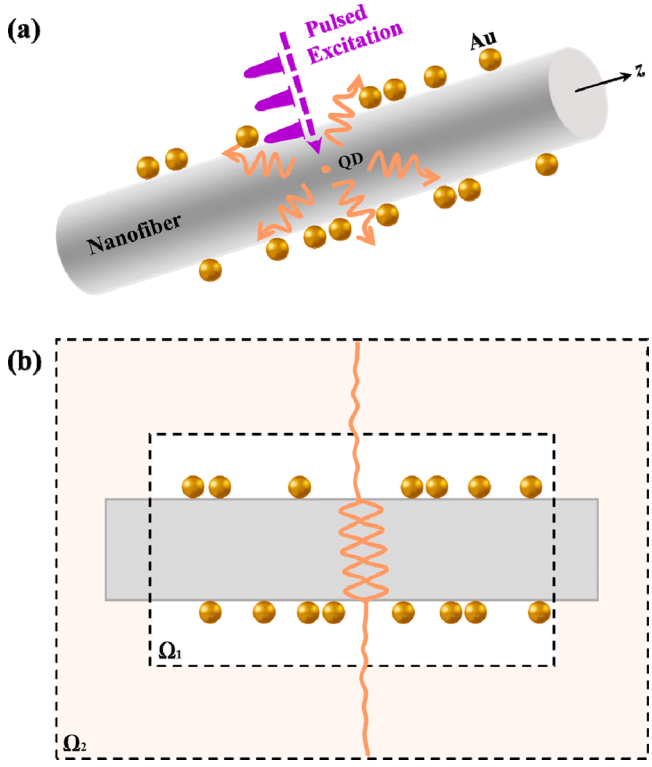

Figure 1. (a) Schematic representation of the excitation of a CdTe QD-doped nanofiber, which is coated with gold nanoparticles and (b) QNM bound by PML.

photonic-plasmonic nanoresonator causes a decrease in the emission rate. As a matter of fact, V is purely an electromagnetic property, which is rather difficult to define for leaky dielectric cavities. Thus, the expression of the usual mode volume requires to be modified for the modes of a nonconservative photonic structure, which are so-called quasi-normal modes (QNM). In this way, using the total electromagnetic field $(\tilde{\mathbf{E}},\tilde{\mathbf{H}})$ generated by a dipole coupled into a single resonance, the mode volume is determined for both real and imaginary parts, which represents the stationary electromagnetic waves and the energy dissipation outside the resonator, respectively, as given by eq 2:[20]

$$V = \frac{\int\left[\tilde{\mathbf{E}}\cdot\frac{\partial(\omega\varepsilon)}{\partial\omega}\tilde{\mathbf{E}} - \tilde{\mathbf{H}}\cdot\frac{\partial(\omega\mu)}{\partial\omega}\tilde{\mathbf{H}}\right]\mathrm{d}^3\mathbf{r}}{2\varepsilon_0 n^2[\tilde{\mathbf{E}}(\mathbf{r}_0)\cdot\mathbf{u}]^2} \quad (2)$$

In this expression, a linearly polarized dipole $\mathbf{p} = p\mathbf{u}$ with a unit vector, $\mathbf{u}$, is considered. ε_0 is the permittivity of the vacuum, ω is the frequency of the dipole in the resonator, ε and μ are the permittivity and permeability values of the photonic structure, respectively.

The electromagnetic field distribution and the mode volume of the hybrid photonic-plasmonic nanoresonator proposed here are determined by time-domain calculations using perfectly matched layers (PMLs). As shown in Figure 1b, the mode volume of the hybrid photonic-plasmonic resonator is calculated over the entire space, including real space, Ω_1, and the surrounding perfectly matched-layer (PML), Ω_2. The main function of the PML is to provide an ongoing electromagnetic field outside the boundary of the photonic cavity. The other crucial function of the PML is to ensure a complex coefficient, which directs the QNM to decrease exponentially through the

DOI: 10.1021/acs.jpcc.9b05289
J. Phys. Chem. C 2019, 123, 19862−19870

PML and to make it disappear at the PML's outer boundaries. Thus, using PML ensures calculations of the exact field distribution and mode volume of the QNM of the photonic structure.

For situations beyond a perfect mode coupling in a dielectric photonic cavity, additional terms are also incorporated to the Purcell factor to reveal the exact changes in the emission rate. For instance, spectral and spatial mismatches between the dipole wavelength, λ, and the cavity resonant wavelength, λ_c, result in modifications in the mode-field distribution, causing a decrease in the spontaneous decay rate. The reductions in the emission rate caused by the spectral and spatial mismatches of the dipole with respect to the optical mode are introduced in the second and third terms of eq 3, respectively, in which $E(r)$ is the electric field amplitude of the optical mode with respect to the location of the dipoles of the CdTe QDs, and the maximum electric field is given by $E_m = (h\nu/2\varepsilon_0 n^2 V)^{1/2}$. An orientation mismatching of the dipole corresponding to the polarization of the optical mode, which is symbolized by η, also induces a decrease in the spontaneous emission rate of a quantum emitter.[21] Thus, the spontaneous emission rate of a quantum emitter for any conservative or dissipative photonic cavity is revised as[20]

$$\frac{\Gamma}{\Gamma_0} = F_p \frac{{\omega_0}^2}{\omega^2} \frac{{\omega_0}^2}{{\omega_0}^2 + 4Q^2(\omega - \omega_0)^2} \frac{|E(\vec{r})|^2}{|E_m|^2} \eta^2 \left[1 + 2Q \frac{\omega - \omega_0}{\omega_0} \frac{Im(V)}{Re(V)}\right] \quad (3)$$

where ω_0 is the vacuum frequency of the dipole.

3. EXPERIMENTAL SECTION

3.1. Materials. Tetrachloroauric(III) acid trihydrate ($HAuCl_4 \cdot 3H_2O$, 99%, Sigma-Aldrich), trisodium citrate dihydrate (≥99%, Sigma-Aldrich), poly(acrylic acid) (PAA, M_w, 1.8 kg/mol, Sigma-Aldrich), poly(vinyl alcohol) (PVA, M_w, 30−70 kg/mol, Sigma-Aldrich, 87−90% hydrolyzed), ethanol (99.9% Abs., Merck) are purchased and used as received without any further purification. The deionized water (18.2 MΩ cm^{-1} at 25 °C) used in extraction is produced by a Milli-Q Advantage water treatment system.

3.2. Methods. *3.2.1. Synthesis of Gold Nanoparticles.* To obtain gold nanoparticles, a typical reduction procedure is followed. Briefly, an aqueous solution of $HAuCl_4$ (0.24 mM, 200 mL) is loaded in a glass container and is heated to reflux under vigorous stirring. Thereafter, trisodium citrate solution (0.34 M, 1 mL) is immediately loaded into the container. The solution is allowed to reflux for 30 min while its color transforms from pale yellow to ruby red due to the reduction of Au^{3+} to Au^0. The final mixture is centrifuged (13 000 rpm, 15 min) and redispersed in 15 mL of ethanol. Individual gold nanoparticles on the surface of the polymer nanofibers are clearly seen in Figure 3b. The average diameter of the nanoparticles is determined to be approximately 20 nm.

3.2.2. Synthesis of CdTe QDs. CdTe QDs were synthesized in aqueous solution by modifying the one-pot method.[22] To prepare cadmium precursor solution, 2.29 g of $CdCl_2$ (s) is dissolved in 440 mL of ultrapure water and 1.68 mL of thioglycolic acid is added to the aqueous cadmium chloride solution. To obtain a transparent cadmium precursor solution, 1 M NaOH (aq) is added until the pH of the precursor solution reaches 11. This precursor solution is degassed with nitrogen gas and heated up to 80 °C with vigorous stirring for 1 h. Meanwhile the tellurium source, NaHTe, is prepared using Te powder (90 mg) and $NaBH_4$ (60 mg) mixed with water (10 mL) under a nitrogen atmosphere. The solution is transferred into a two-necked flask and heated up to 60 °C while bubbled with N_2 to purge oxygen in the medium completely. The Te precursor solution is heated up to 60 °C until H_2 (g) formation is completed, indicating the formation of NaHTe. This solution is quickly mixed with the cadmium precursor solution, and the reaction temperature is raised up to 110 °C. As soon as the temperature reaches 110 °C, aliquots are taken to observe the growth of the QDs. CdTe QD formation is monitored by UV−vis absorption and PL spectroscopic measurements as well as directly observing color of the solution under UV light. The growth of QDs is also tracked by dynamic light scattering (DLS) measurements by taking aliquots while the reaction progresses. The reaction is stopped by cooling the solution when the desired particle size and emission color are reached. The slower growth ensures formation of highly luminescent CdTe QDs dispersed in water. The QDs are precipitated by adding 2-propanol into the solution and redispersed in water. The precipitation procedure is repeated several times to purify QDs from all impurities. The average diameter of the CdTe QDs used in the experiments is determined to be approximately 7 nm. Normalized UV−vis absorption and photoluminescence emission spectra of CdTe QDs and absorption spectrum of gold nanoparticles are given in Figure 2.

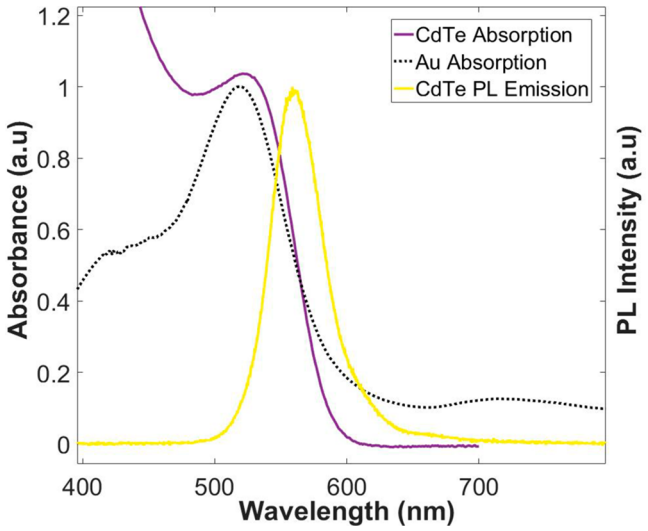

Figure 2. Absorbance and photoluminescence emission spectra of CdTe QDs and absorbance spectrum of the individual gold nanoparticles.

3.2.3. Fabrication of Electrospun Nanofibers. The CdTe containing gold nanoparticle-coated electrospun polymer nanofibers are fabricated using the electrospinning method. CdTe nanoparticles (60 μL) are dispersed into polymer solution (28.75% w/v, in 1 mL of water). The electrospinning of this suspension is carried out onto an aluminum foil collector to obtain fiber morphology. The relative polymer ratio in solution is kept as 4:1 (PVA/PAA). Two electrode holders are connected to the syringe needle and the collector. A fixed potential of 15 kV is applied while the flow rate and the distance is set to 0.3 mL/h and 15 cm, respectively. Afterward,

DOI: 10.1021/acs.jpcc.9b05289
J. Phys. Chem. C 2019, 123, 19862−19870

the resulting polymer blend in fiber morphology is cross-linked through heating at 90 °C for 30 min. For metal nanoparticle coating onto fiber surfaces, the cross-linked fibers are immersed into a gold nanoparticle mixture for 2 h. The gold nanoparticle-coated fibers is then washed by ethanol to remove free nanoparticles from the system and dried under vacuum for 2 h. The scanning electron microscopy (SEM) image of the uncoated electrospun polymer nanofibers is shown in Figure 3a. SEM pictures of the nanofibers decorated by individual

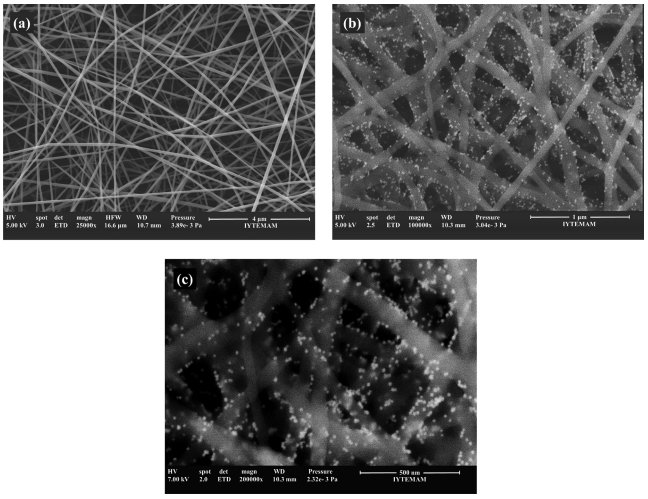

Figure 3. SEM images of the (a) polymer nanofibers and gold nanoparticle-coated electrospun polymer nanofibers at different scales: (b) 1 μm and (c) 500 nm.

gold nanoparticles at different scales, 1 μm and 500 nm, are shown in Figure 3b,c, respectively. The diameters of the individual nanofibers are determined to be approximately 100 nm, as seen in Figure 3c.

3.3. Time-Resolved Fluorescence Lifetime Measurements. Time-resolved experiments are carried out to investigate fluorescence lifetime of QDs confined in nanofibers using an optical setup illustrated in Figure 4. A TimeHarp 200

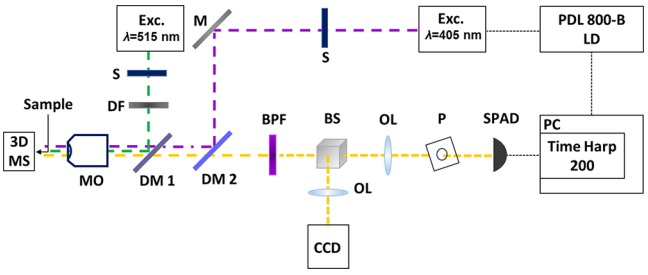

Figure 4. Time-resolved fluorescence lifetime spectroscopy setup.

PC-Board system (Picoquant, GmbH) is operated for time-correlated measurements. CdTe QDs doped polymer nanofibers are repeatedly excited through their lateral surfaces with pulses using a picosecond pulsed diode laser at a wavelength of 405 nm with a repetition frequency of 10 MHz (LDH-D-C-405 Picoquant, GmbH), reflecting from the mirror (M), and a PDL 800-B laser driver is used to activate the laser beam. An objective lens (OL) with a numerical aperture of 0.70 (Nikon ELWD 100×) and a working distance of 10.1 mm is utilized to focus the excitation light reflecting from the dichroic mirror (DM 2) onto the sample and to accumulate the photoluminescence from the excited QDs. A band-pass filter (BPF) is used to completely eliminate the excitation light, and an optical pinhole (P) is placed to the focal plane to remove the out of focus light. The fluorescence signal is split by a beam splitter (BS) and is sent onto a CCD camera, Optronis-1836-ST-153, and a single-photon avalanche diode photodetector (SPAD) to detect the emitted photons from the excited samples; thereafter, single photon events are accumulated to record the time delay between short excitation pulses and the detected photons. Fluorescence decay curves are obtained by the time-dependent histogram data, and a FluoFit computer program is utilized to determine the fluorescence decay curves, τ_1 and τ_2, with their rate percent values, amplitude-averaged ($\langle\tau^a\rangle$) and intensity-averaged (τ^b) lifetimes, which are given in detail,[23] minimizing the fitting parameter (χ^2). In our experiments, localized surface plasmons on the gold nanoparticle clusters are monitored by a CCD camera under high excitation power. A pulsed laser at the wavelength of 515 nm with a repetition rate of 30 Hz (Flare NX 515-0.6-2 Coherent) is operated to pump the CdTe QDs confined in the gold nanoparticle-decorated photonic structures, and a reflective neutral density filter (DF) is employed to arrange the excitation intensity. The same microscope objective is used to focus the excitation light from the dichroic mirror (DM 1), which is mounted onto a flip head, onto the sample and to collect the photoluminescence from the QDs. After localized plasmons on the surface of the accumulated gold nanoparticles are monitored as a hotspot, the high-power laser beam is blocked by a shutter (S) and the time-resolved experiments are performed to analyze the fluorescence lifetimes of the CdTe QDs at these hotspots.

4. RESULTS

Figure 5 shows the distinctive characteristics in the decay populations of the fluorescence emission from CdTe QDs in

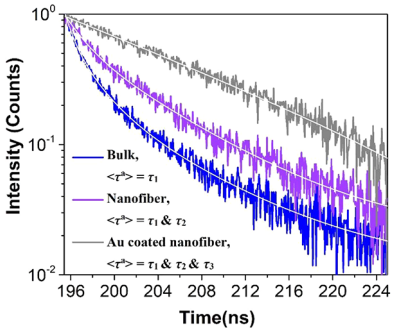

Figure 5. Fluorescence decay curves of the excited CdTe QDs in the bulk polymer, bare nanofiber, and in nanofiber coated with gold nanoparticles.

bulk, bare nanofiber, and gold nanoparticle-decorated nanofiber media. The average fluorescence lifetime of the QDs in bulk phenol is determined to be 15.10 ns, using a single exponential decay fit. The total fluorescent emission from the excited QDs in nanofibers stems from both the resonant and nonresonant emitted light. The resonant light emission corresponds to the fastest decay component of the total photoluminescence (PL) since the vacuum fluctuations increase and, henceforth, enhance the transition rate of the photon populations as the radiation from the dipole is coupled into the resonant optical mode. However, some portion of the

DOI: 10.1021/acs.jpcc.9b05289
J. Phys. Chem. C 2019, 123, 19862−19870

Table 1. Experimental Fluorescence Decay Rate Parameters of CdTe QDs in Bulk, Uncoated Nanofiber (nf), and Coated Nanofiber (Coated nf) Cavities

sample	τ_1 (ns)	τ_1 (%)	τ_2 (ns)	τ_2 (%)	τ_3 (ns)	τ_3 (%)	$\langle\tau^a\rangle$ (ns)	τ^b (ns)	χ^2	Γ/Γ_0
bulk	15.10	100							1.05	
nf 1	15.04	36.71	4.16	63.29			8.15	11.53	0.95	3.6
nf 2	13.97	49.78	4.03	50.22			8.98	11.72	0.97	3.7
nf 3	14.19	38.26	4.09	61.74			7.96	10.99	0.95	3.7
nf 4	15.74	36.51	4.32	63.49			8.49	12.05	0.96	3.5
nf 5	15.65	51.18	4.46	48.82			10.19	13.26	0.98	3.4
coated nf 1	15.19	10.19	4.62	39.44	1.22	50.37	3.98	8.21	0.96	12.4
coated nf 2	12.50	17.64	4.08	31.81	1.42	50.55	4.22	8.03	0.97	10.6
coated nf 3	11.82	16.31	3.53	41.13	1.52	42.56	4.03	7.18	0.98	9.9
coated nf 4	16.31	15.10	4.25	36.81	1.28	48.08	4.64	10.25	0.99	11.8
coated nf 5	14.23	12.22	4.00	34.26	1.31	53.52	3.81	8.17	0.99	11.5

PL stems from the uncoupled emission because of the fact that the dipoles of the CdTe QDs are randomly oriented and the photonic cavity proposed here is assumed to be a leaky photonic structure with a low Q-factor. Thus, the fluorescence emission from the encapsulated QDs in nanofibers is analyzed using two exponential decay components that correspond to nonresonant and resonant emission parts, τ_1, which is measured to be approximately 14.92 ns, and τ_2, which is measured to be 4.21 ns, respectively. Thus, the average spontaneous emission rate of the CdTe QDs coupled into the optical nanofibers is determined to enhance by a factor of 3.6, based on the time-resolved fluorescence lifetime measurements. Because the diameter of the electrospun nanofibers is determined to be approximately 100 nm and the total photoluminescence (PL) stems from the excitation of the encapsulated CdTe QDs by a laser beam with a spot size of about 700 nm, the fluorescence emission is collected by the QDs in various nanofibers, which have almost the same physical and optical properties. Thus, the measured emission signal contains the fluorescence lifetimes coming at least from several nanoresonators. Table 1 shows the fluorescence emission decay parameters (τ_1 and τ_2) of the QDs, together with their percentage values obtained by the excitation of five different regions of the same coated and uncoated nanofiber samples. Since the average value of each decay parameter is obtained, the results are revealed to be quite similar.

As gold nanoparticle-decorated nanofibers are excited with the pulse laser, gold nanoparticles make the surface plasmons available to enhance the electric field intensity at deep subwavelength regions and intense local electromagnetic fields are coupled into the optical mode of nanofibers, regenerating the mode field distribution inside the photonic-plasmonic nanostructures. Time-resolved experimental results demonstrate that although fluorescence decay curves include the emission from nonresonant (τ_1) and resonant cavity modes of the optical fiber, which are not affected by the presence of the gold nanoparticles (τ_2), some portion of the photon population is coupled into the hybrid photonic-plasmonic mode, giving an additional fluorescence lifetime, i.e., τ_3, since the fluorescence emission from the encapsulated QDs is localized with increased density of electromagnetic states by plasmonic nanoantennas. Thus, a three-exponential decay fit procedure is employed to obtain the fluorescence lifetime of the emitters in gold nanoparticle-coated nanofibers. The fluorescence intensity is determined by the following expression:

$$I = I_1 \exp[-(t - t_0)/\tau_1] + I_2 \exp[-(t - t_0)/\tau_2] + I_3 \exp[-(t - t_0)/\tau_3] \quad (4)$$

The fluorescence lifetime measurements of CdTe QDs interacting with distinct gold nanoparticles in the hybrid photonic-plasmonic nanostructures show that τ_3 decreases to a value of 1.35 ns, which corresponds to the highest percentage value for the total fluorescence emission. Nonetheless, the fluorescence decay curves obtained from the other parts of the fluorescence emission, that is, τ_1 and τ_2, are observed to remain almost unchanged with their moderate percentages as seen in Table 1. Thus, the average spontaneous emission rate of the encapsulated emitters coupled into the hybrid mode is determined to enhance by a factor of 11.2, which is approximately 3 times greater than that of the uncoated nanofibers one.

It is noticed that the gold nanoparticles, decorated on the outer surface of the nanofibers, act like absorptive cavity mirrors, which are observed to cause a decrease in the photoluminescence intensity of the QDs because of the radiation loss at the surface of the plasmonic nanostructures. However, since the nanofibers are not entirely covered by the gold nanoparticles, the loss is measured to be not more than 30%. On the other hand, for some spots of the partially coated nanofibers, which consists of gold nanoparticle clusters, as shown in Figure 7a, an enormous enhancement of the PL intensity at hot electromagnetic zones is recorded, approximately 10 times greater than that of the uncoated nanofibers' one.

A 3D finite difference time domain (FDTD) technique is utilized to acquire the electric field patterns of the fluorescing CdTe QDs, which are coupled into an optical nanofiber cavity. The perspective view of the hybrid nanostructure in numerical calculations is given in Figure 6a.

In the simulations, the corresponding diameter and refractive index parameters of the polymer nanofibers, which are made of PVA and PAA, are utilized. A single nanofiber is taken to be aligned with the z-axis, with a length of 3 μm to be considered as infinitely long compared to the fiber diameter of 100 nm. Randomly distributed electric dipoles are placed in the photonic structure, which are aligned with the z-axis. The mesh grid size enclosing the hybrid structure is determined to be 1 nm, and the thickness of the PML is specified to be 430 nm with respect to the 1 nm grid size, which is large enough for QNM to decay exponentially and vanish at the PML's outer boundaries. The perspective and top views of the electric field distribution profiles of the QDs confined in the polymer

DOI: 10.1021/acs.jpcc.9b05289
J. Phys. Chem. C 2019, 123, 19862−19870

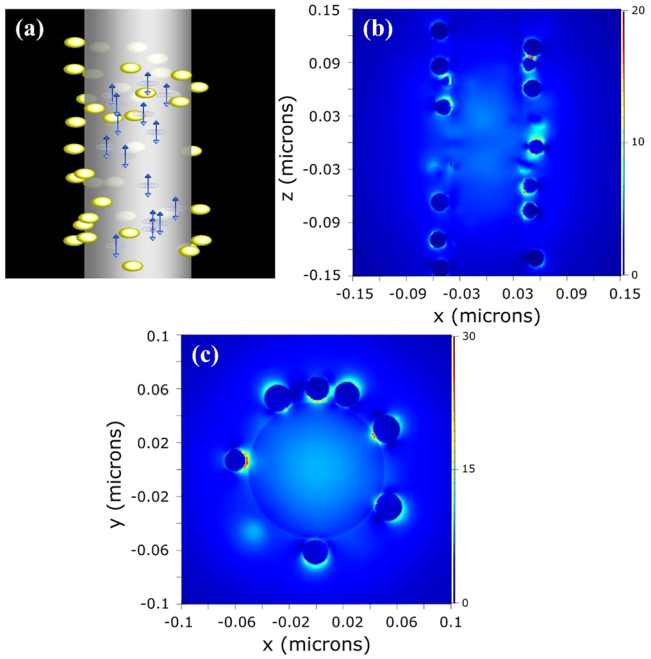

Figure 6. (a) Perspective view of the hybrid nanostructure. (b) Perspective and (c) top views of the electric field distribution profile of the QDs confined in the nanofiber, decorated by individual gold nanoparticles.

nanofiber that are partially coated with discrete gold nanoparticles are given in Figure 6b,c, respectively. The magnified local optical fields around the metal nanoparticles, which are evidence of the changes in the density of the electromagnetic states, are clearly demonstrated in the simulation pictures.

The changes in the spontaneous emission rate of the encapsulated QDs, coupled to uncoated and partially coated nanofibers, are also determined by eq 3. The spectral, spatial, and orientation mismatches between the dipole and cavity mode are taken into consideration in order to calculate the theoretical enhancement factor given by eq 3.[24] For instance, spectral averaging of the second term in eq 3 gives a factor of 1/2 and the average value of the third term is found to be approximately 1/3 for uniformly distributed dipoles of CdTe QDs. For randomly oriented dipoles, the orientation mismatching of the dipole of the QDs with respect to the polarization of the cavity mode is determined to be equal to 1/3.[21] *Q*-factor and mode volume values for the nanoresonators are obtained by the FDTD calculations. Since the hybrid photonic design studied here is assumed to be in the regime of a low *Q*-factor, the imaginary part of the mode volume, which corresponds to the energy dissipation of the photonic cavity, is also considered in the spontaneous emission rate enhancement factor given by eq 3. As the real part of the mode, the volume in the uncoated nanofiber is obtained to be $V_{re} = 0.14(\lambda/n)^3 \times 10^{-4}$, and the imaginary part is found to be insignificant, which is equal to a mode volume of $V_{im} = 0.48i(\lambda/n)^3 \times 10^{-9}$. However, since the loss caused by the individual gold nanoparticles is determined to be considerable using the Drude model for electric permittivity,[20] the imaginary part of the mode volume is found to be significant for partially gold nanoparticle-decorated nanofibers, which results in a total mode volume of $V = (4.03 - 0.32i)(\lambda/n)^3 \times 10^{-6}$. Such an enormous amount of decrease in the total mode volume in the hybrid photonic-plasmonic nanoresonator is attributed to the occurrence of the intense light localization by distinct gold nanoparticles that couple into the hybrid optical mode of the nanofiber, resulting in the enhanced spontaneous emission rate of CdTe QDs. The *Q*-factor for coated and uncoated nanofiber photonic nanoresonators are found to be slightly different, which is determined to be 9 and 16, respectively. Thus, the theoretical enhancement factors, Γ/Γ_0, of the nanofiber and the hybrid photonic-plasmonic nanoresonator are found to be approximately 2.7 and 10.1, respectively, which confirm that there is a good agreement between the theoretical and experimental results obtained for the spontaneous emission rate in our photonic-plasmonic nanocavities.

In our samples, although nanofiber structures are partially coated by distinct gold nanoparticles and excitation of different regions of the same sample are determined to give quite similar enhancement factors, nevertheless, some clusters of the gold nanoparticles are also observed to generate hot electromagnetic zones upon excitation of the samples using a high-power laser. The localized plasmon modes around these gold clusters are detected by a CCD camera through shining electromagnetic field spots using the optical setup illustrated in Figure 4; thereafter, the time-resolved experiments are performed to investigate the changes in the spontaneous emission rate of the encapsulated CdTe QDs. Figure 7a demonstrates the perspective view of the nanostructure surrounded by a gold nanoparticle cluster. The top view of the electric field distribution profile of the QDs confined in the nanofiber that is in contact with a gold nanoparticle cluster is demonstrated in Figure 7b. A hot electromagnetic field zone around the cluster is noticeably seen in the simulation picture.

Our experimental results on the modification of the spontaneous emission rate of CdTe QDs in nanofiber cavities covered by gold nanoparticle clusters at six different regions are given in Table 2. Although fluorescence emission from the encapsulated CdTe QDs is analyzed using two exponential decay components, a great majority of the fluorescence signal comes from the fast decay rate arising from the coupling of the photons into deep subwavelength regions of the gold nanoparticle clusters, as seen in the percentage values of the

Table 2. Experimental Fluorescence Decay Rate Parameters of CdTe QDs in Nanofiber Cavities Covered by Gold Nanoparticle Clusters

gold cluster	τ_1 (ns)	τ_1 (%)	τ_2 (ns)	τ_2 (%)	$\langle\tau^a\rangle$ (ns)	τ^b (ns)	χ^2	Γ/Γ_0
1	2.79	5.15	0.72	94.85	0.83	1.08	1.02	21.0
2	4.53	3.82	0.91	96.18	1.05	1.51	0.98	16.6
3	4.47	3.59	0.77	96.41	0.90	1.43	1.03	19.6
4	4.11	6.93	0.75	93.07	0.99	1.72	0.99	20.3
5	3.52	5.95	0.74	94.05	0.91	1.38	0.98	20.4
6	3.67	5.19	0.81	94.81	0.96	1.38	1.03	15.7

DOI: 10.1021/acs.jpcc.9b05289
J. Phys. Chem. C 2019, 123, 19862−19870

fluorescence lifetimes given in Table 2. Slight variations in the experimental data are attributed to be due to the different sizes of the gold nanoparticle clusters on the surface of the nanofibers. Figure 7c shows the fluorescence decay curve of

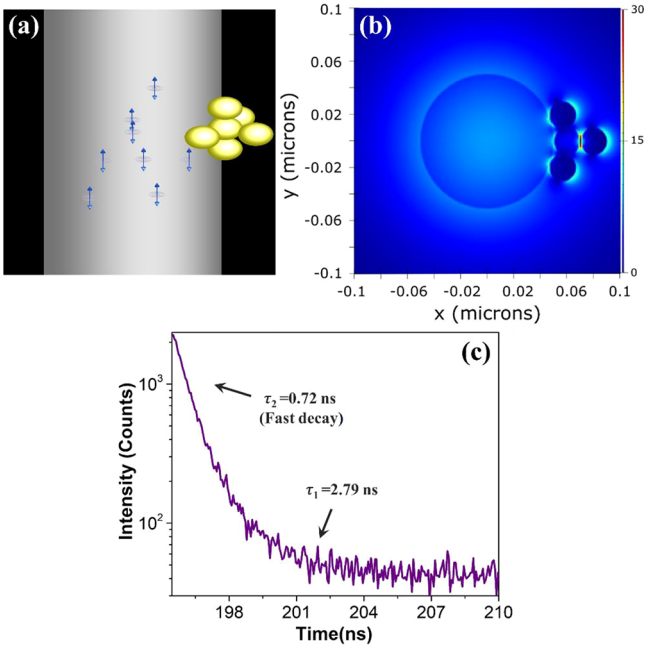

Figure 7. (a) Perspective view of the nanostructure surrounded by gold nanoparticle cluster. (b) Top view of the electric field distribution profile of the QDs confined in the nanofiber surrounded by a gold nanoparticle cluster. (c) Fluorescence decay curve of the excited CdTe QDs in an optical nanofiber covered by a gold nanoparticle cluster.

CdTe QDs in a polymer nanofiber, which is in contact with a gold nanoparticle cluster, as seen by Figure 7a, whose fast decay is measured to be 0.72 ns, and other related details of the decay parameters are given in Table 2. Experimental results demonstrate that remarkable spontaneous emission rate enhancement factors are accomplished for the encapsulated QDs, ranging from 15.7 to 21.0, depending upon the size of the gold nanoparticle clusters. Theoretical enhancement factor for such a determined cluster illustrated in Figure 7 is also calculated using eq 3. A mode volume of $V = (1.38 - 0.11i)(\lambda/n)^3 \times 10^{-6}$ and a Q-factor of 7.5 are determined by FDTD calculations, which yield an enhancement factor of 15.3 for the spontaneous emission rate. These results evidently confirm that gold nanoparticle clusters can be utilized in a hybrid photonic-plasmonic system to significantly enhance the density of electromagnetic states in the vicinity of quantum emitters.

Although our experimental results are confirmed to be in good agreement with the theoretical calculations obtained via the model introduced by eq 3, in fact, in QDs and gold nanoparticles systems, which is a representative of semiconductor-metal hybrid nanostructures, gold nanoparticles can behave as the efficient energy acceptors and are able to quench the fluorescence emission energy of the donors due to nanosurface energy transfer (NSET) or fluorescence resonance energy transfer (FRET) processes. Therefore, we envisage that one may not totally eliminate the effects of these quenching mechanisms since some of the QDs are possibly located at very close proximity to the fiber's outer surface, being almost in contact with some of the gold nanoparticles. Consistency between the experimental and theoretical results suggest that the physical mechanism affecting the spontaneous emission rate of the encapsulated QDs in such a hybrid photonic-plasmonic nanoresonator is assumed to be mainly due to the regeneration of the mode field in the nanofiber cavity upon the interaction of the dipoles with the surface plasmons of distinctive gold nanoparticles that surround the outer surface of the nanofiber. Therefore, NSET and FRET mechanisms are assumed to have negligible effects on the gold-coated nanofiber system studied here in this work.

5. DISCUSSION

Research on light−matter interactions in photonic cavities has been of great importance in many research fields, serving as a bridge between classical and quantum physics and opening new avenues with extensive applications in quantum information technologies, integrated and nonlinear optics, and optical imaging.[25−28] Photonic resonators are capable of altering the localized density of the optical states in regions of the wavelength scale where the emission frequency of the emitter is tuned to one of the photonic cavity's fundamental modes.[29,30] Improving the photon-radiation efficiency and the spontaneous decay rate of the confined light emitters in photonic cavities can elegantly allow controlling the fundamental properties of light emitting quantum optical devices such as nanolasers[31] and single-photon sources.[32] The physical dynamics behind high-quality nanoscale lasers and other photonic sources have been elucidated in various studies to be employed in some novel device applications with enhanced performances.[33−35] For instance, recently, light−matter interaction in Perovskite nanowires has been analyzed by studying of exciton-photon interactions in the directional optical structures to investigate the origin of the lasing modes with high Q-factors and low pumping thresholds.[36]

Great advances in the area of the cavity quantum electrodynamics (QED) have been accomplished through employing different kinds of well-designed dielectric photonic cavities, some of which have ultrahigh Q-factors, such as photonic crystals,[37] micropillars,[38] or whispering gallery-mode (WGM) microresonators;[39] nevertheless, the mode volume of these structures is beyond the subwavelength scale for the purpose of the deep confinement of the electromagnetic waves.[40] Electrospun polymer nanofibers have been demonstrated to have an outstanding potential to manipulate the vacuum fluctuations of the encapsulated dye molecules resulting from the dielectric material properties and the confinement of the optical modes in suitable optical dimensions.[41] Although the nanofibers can be produced in desired dimensions on the order of subwavelengths to originate photonic structures with a small mode volume, the light−matter interaction in these moderate resonators is considered to be limited because of their low Q-factors. In this work, for the first time, CdTe QD-doped electrospun polymer nanofibers are coated with discrete gold nanoparticles of about 20 nm in diameters to construct low-Q hybrid photonic-plasmonic nanoresonators that are considered to be smart, stable, and reproducible in order to improve the emission dynamics of the encapsulated QDs. We envisage that such a kind of hybrid mode based mechanism proposed in this work enables investigating light−matter interactions further in photonic-plasmonic nanoresonators, which might be promising

DOI: 10.1021/acs.jpcc.9b05289
J. Phys. Chem. C 2019, 123, 19862−19870

for achieving new designs of simple low-Q hybrid photonic devices to dramatically alter the spontaneous emission rate.

6. CONCLUSION

In this paper, the fluorescent dynamics of CdTe QDs, encapsulated by polymer nanofibers, which are partially coated by distinct gold nanoparticles, are investigated by a time-resolved spectroscopic technique. As light emission from the excited QDs is coupled into the hybrid photonic-plasmonic mode, the spontaneous emission rate of the fluorescent emitters is observed to enhance by a factor of 11.2, which is about 3 times greater than that of the decay rate measured for uncoated CdTe QD-doped nanofibers. Our study reveals that using such gold nanoparticle-decorated electrospun polymer nanofibers enable obtaining low-Q hybrid photonic-plasmonic nanoresonators to significantly alter the spontaneous emission rate of the encapsulated quantum emitters.

AUTHOR INFORMATION

Corresponding Author

*E-mail: naci.inci@boun.edu.tr.

ORCID

Serdar Ozcelik: 0000-0003-2029-0108

Mustafa M. Demir: 0000-0003-1309-3990

M. Naci Inci: 0000-0002-3384-3683

Notes

The authors declare no competing financial interest.

ACKNOWLEDGMENTS

Belkıs Gökbulut acknowledges the Boğaziçi University Research Fund for the financial support provided under Contract Number 14240.

REFERENCES

(1) De Leon, N. P.; Shields, B. J.; Yu, C. L.; Englund, D. E.; Akimov, A. V.; Lukin, M. D.; Park, H. Tailoring Light-Matter Interaction with a Nanoscale Plasmon Resonator. *Phys. Rev. Lett.* **2012**, *108*, 226803.

(2) Chikkaraddy, R.; De Nijs, B.; Benz, F.; Barrow, S. J.; Scherman, O. A.; Rosta, E.; Demetriadou, A.; Fox, P.; Hess, O.; Baumberg, J. J. Single-Molecule Strong Coupling at Room Temperature in Plasmonic Nanocavities. *Nature* **2016**, *535*, 127−130.

(3) Gu, Y.; Wang, L.; Ren, P.; Zhang, J.; Zhang, T.; Martin, O. J. F.; Gong, Q. Surface-Plasmon-Induced Modification on the Spontaneous Emission Spectrum via Subwavelength-Confined Anisotropic Purcell Factor. *Nano Lett.* **2012**, *12*, 2488−2493.

(4) Kongsuwan, N.; Demetriadou, A.; Chikkaraddy, R.; Benz, F.; Turek, V. A.; Keyser, U. F.; Baumberg, J. J.; Hess, O. Suppressed Quenching and Strong-Coupling of Purcell-Enhanced Single-Molecule Emission in Plasmonic Nanocavities. *ACS Photonics* **2018**, *5*, 186−191.

(5) Schuller, J. A.; Barnard, E. S.; Cai, W.; Jun, Y. C.; White, J. S.; Brongersma, M. L. Plasmonics for Extreme Light Concentration and Manipulation. *Nat. Mater.* **2010**, *9*, 193−2014.

(6) Huang, S.; Ming, T.; Lin, Y.; Ling, X.; Ruan, Q.; Palacios, T.; Wang, J.; Dresselhaus, M.; Kong, J. Ultrasmall Mode Volumes in Plasmonic Cavities of Nanoparticle-On-Mirror Structures. *Small* **2016**, *12*, 5190−5199.

(7) Lu, Y.-J.; Wang, C.-Y.; Kim, J.; Chen, H.-Y.; Lu, M.-Y.; Chen, Y.-C.; Chang, W.-H.; Chen, L.-J.; Stockman, M. I.; Shih, C.-K.; et al. All-Color Plasmonic Nanolasers with Ultralow Thresholds: Autotuning Mechanism for Single-Mode Lasing. *Nano Lett.* **2014**, *14*, 4381−4388.

(8) Sugimoto, H.; Yashima, S.; Fujii, M. Hybridized Plasmonic Gap Mode of Gold Nanorod on Mirror Nanoantenna for Spectrally Tailored Fluorescence Enhancement. *ACS Photonics* **2018**, *5*, 3421−3427.

(9) Ji, B.; Giovanelli, E.; Habert, B.; Spinicelli, P.; Nasilowski, M.; Xu, X.; Lequeux, N.; Hugonin, J.-P.; Marquier, F.; Greffet, J.-J.; et al. Non-Blinking Quantum Dot with a Plasmonic Nanoshell Resonator. *Nat. Nanotechnol.* **2015**, *10*, 170−175.

(10) Hill, M. T.; Oei, Y.-S.; Smalbrugge, B.; Zhu, Y.; de Vries, T.; van Veldhoven, P. J.; van Otten, F. W. M.; Eijkemans, T. J.; Turkiewicz, J. P.; de Vaardt, H.; et al. Lasing in metallic-coated nanocavities. *Nat. Photonics* **2007**, *1*, 589−594.

(11) Weeber, J.-C.; Bouhelier, A.; Colas des Francs, G.; Markey, L.; Dereux, A. Submicrometer In-Plane Integrated Surface Plasmon Cavities. *Nano Lett.* **2007**, *7*, 1352−1359.

(12) Schmidt, M. A.; Lei, D. Y.; Wondraczek, L.; Nazabal, V.; Maier, S. A. Hybrid Nanoparticle−Microcavity-Based Plasmonic Nanosensors with Improved Detection Resolution and Extended Remote-Sensing Ability. *Nat. Commun.* **2012**, *3*, 1108.

(13) Liu, J.-N.; Huang, Q.; Liu, K.-K.; Singamaneni, S.; Cunningham, B. T. Nanoantenna−Microcavity Hybrids with Highly Cooperative Plasmonic−Photonic Coupling. *Nano Lett.* **2017**, *17*, 7569−7577.

(14) Barth, B.; Schietinger, S.; Fischer, S.; Becker, J.; Nüsse, N.; Aichele, T.; Löchel, B.; Sönnichsen, C.; Benson, O. Nanoassembled Plasmonic-Photonic Hybrid Cavity for Tailored Light-Matter Coupling. *Nano Lett.* **2010**, *10*, 891−895.

(15) Doeleman, H. M.; Verhagen, E.; Koenderink, A. F. Antenna−Cavity Hybrids: Matching Polar Opposites for Purcell Enhancements at Any Linewidth. *ACS Photonics* **2016**, *3*, 1943−1951.

(16) Xiao, Y.-F.; Liu, Y.-C; Li, B.-B; Chen, Y.-L.; Li, Y.; Gong, Q. Strongly Enhanced Light-Matter Interaction in a Hybrid Photonic-Plasmonic Resonator. *Phys. Rev. A: At., Mol., Opt. Phys.* **2012**, *85*, No. 031805.

(17) Purcell, E. M. Spontaneous Emission Probabilities at Radio Frequencies. *Phys. Rev.* **1946**, *69*, 681.

(18) Romeira, B.; Fiore, A. Purcell Effect in the Stimulated and Spontaneous Emission Rates of Nanoscale Semiconductor Lasers. *IEEE J. Quantum Electron.* **2018**, *54*, 2000412.

(19) Gérard, J. M.; Sermage, B.; Gayral, B.; Legrand, B.; Costard, E.; Thierry-Mieg, V. Enhanced Spontaneous Emission by Quantum Boxes in a Monolithic Optical Microcavity. *Phys. Rev. Lett.* **1998**, *81*, 1110−1113.

(20) Sauvan, C.; Hugonin, J. P.; Maksymov, I. S.; Lalanne, P. Theory of the Spontaneous Optical Emission of Nanosize Photonic and Plasmon Resonators. *Phys. Rev. Lett.* **2013**, *110*, 237401.

(21) Gérard, J. M.; Gayral, B. Strong Purcell Effect for InAs Quantum Boxes in Three-Dimensional Solid-State Microcavities. *J. Lightwave Technol.* **1999**, *17*, 2089−2095.

(22) Gu, Z.; Zou, L.; Fang, Z.; Zhu, W.; Zhong, X. One-Pot Synthesis of Highly Luminescent CdTe/CdS Core/Shell Nanocrystals in Aqueous Phase. *Nanotechnology* **2008**, *19*, 135604−135612.

(23) Gökbulut, B.; Inanç, A.; Topcu, G.; Guner, T.; Demir, M. M.; Inci, M. N. Enhancement of the Spontaneous Emission Rate of Perovskite Nanowires Coupled into Cylindrical Hollow Nanocavities Formed on the Surface of Polystyrene Microfibers. *J. Phys. Chem. C* **2019**, *123*, 9343−9351.

(24) Solomon, G. S.; Xie, Z.; Fang, W.; Xu, J. Y.; Yamilov, A.; Cao, H.; Ma, Y.; Ho, S. T. Large Spontaneous Emission Enhancement in InAs Quantum Dots Coupled to Microdisk Whispering Gallery Modes. *Phys. Status Solidi B* **2003**, *238*, 309−312.

(25) Ritter, S.; Nolleke, C.; Hahn, C.; Reiserer, A.; Neuzner, A.; Uphoff, M.; Mucke, M.; Figueroa, E.; Bochmann, J.; Rempe, G. An Elementary Quantum Network of Single Atoms in Optical Cavities. *Nature* **2012**, *484*, 195−200.

(26) Javadi, A.; Söllner, I.; Arcari, M.; Lindskov Hansen, S.; Midolo, L.; Mahmoodian, S.; Kiršanskė, G.; Pregnolato, T.; Lee, E. H.; Song, J. D.; et al. Single-Photon Non-linear Optics with a Quantum Dot in a Waveguide. *Nat. Commun.* **2015**, *6*, 8655.

(27) Kockum, A. F.; Miranowicz, A.; Macri, V.; Savasta, S.; Nori, F. Deterministic Quantum Nonlinear Optics with Single Atoms and

DOI: 10.1021/acs.jpcc.9b05289
J. Phys. Chem. C 2019, 123, 19862−19870

Virtual Photons. *Phys. Rev. A: At., Mol., Opt. Phys.* **2017**, *95*, No. 063849.
(28) Kryuchkyan, G. Y.; Shahnazaryan, V.; Kibis, O. V.; Shelykh, I. A. Resonance Fluorescence from an Asymmetric Quantum Dot Dressed by a Bichromatic Electromagnetic Field. *Phys. Rev. A: At., Mol., Opt. Phys.* **2017**, *95*, No. 013834.
(29) Gökbulut, B.; Inci, M. N. Inhibition of Spontaneous Emission in a Leaky Mode Wedge Nanocavity. *Photonics & Nanostructures: Fundam. Appl.* **2018**, *32*, 68−73.
(30) Gökbulut, B.; Inci, M. N. Enhancement of the Spontaneous Emission Rate of Rhodamine 6G Molecules Coupled into Transverse Anderson Localized Modes in a Wedge-Type Optical Waveguide. *Opt. Express* **2019**, *27*, 15996−16011.
(31) Wu, S.; Buckley, S.; Schaibley, J. R.; Feng, L.; Yan, J.; Mandrus, D. G.; Hatami, F.; Yao, W.; Vučković, J.; Majumdar, A.; et al. Monolayer Semiconductor Nanocavity Lasers with Ultralow Thresholds. *Nature* **2015**, *520*, 69−72.
(32) Hoang, T. B.; Akselrod, G. M.; Mikkelsen, M. H. Ultrafast Room-Temperature Single Photon Emission from Quantum Dots Coupled to Plasmonic Nanocavities. *Nano Lett.* **2016**, *16*, 270−275.
(33) Fraser, M. D.; Höfling, S.; Yamamoto, Y. Physics and Applications of Exciton-Polariton Lasers. *Nat. Mater.* **2016**, *15*, 1049−1052.
(34) Sanvitto, D.; Kénacohen, S. The Road Towards Polaritonic Devices. *Nat. Mater.* **2016**, *15*, 1061−1073.
(35) Wang, X.; Zhou, H.; Yuan, S.; Zheng, W.; Jiang, Y.; Zhuang, X.; Liu, H.; Zhang, Q.; Zhu, X.; Wang, X.; et al. Cesium Lead Halide Perovskite Triangular Nanorods as High-Gain Medium and Effective Cavities for Multiphoton-Pumped Lasing. *Nano Res.* **2017**, *10*, 3385−3395.
(36) Wang, X.; Shoaib, M.; Wang, X.; Zhang, X.; He, M.; Luo, Z.; Zheng, W.; Li, H.; Yang, T.; Zhu, X.; et al. High-Quality In-Plane Aligned CsPbX3 Perovskite Nanowire Lasers with Composition-Dependent Strong Exciton−Photon Coupling. *ACS Nano* **2018**, *12*, 6170−6178.
(37) Asano, T.; Ochi, Y.; Takahashi, Y.; Kishimoto, K.; Noda, S. Photonic Crystal Nanocavity with a Q Factor Exceeding Eleven Million. *Opt. Express* **2017**, *25*, 1769−1777.
(38) Song, H.-Z.; Takemoto, K.; Miyazawa, T.; Takatsu, M.; Iwamoto, S.; Ekawa, M.; Yamamoto, T.; Arakawa, Y. High Quality-Factor Si/SiO2-InP Hybrid Micropillar Cavities with Submicrometer Diameter for 1.55-μm Telecommunication Band. *Opt. Express* **2015**, *23*, 16264−16272.
(39) Lin, G.; Diallo, S.; Henriet, R.; Jacquot, M.; Chembo, Y. K. Barium Fluoride Whispering-Gallery-Mode Disk-Resonator with One Billion Quality-Factor. *Opt. Lett.* **2014**, *39*, 6009−6012.
(40) Yang, K. Y.; Oh, D. Y.; Lee, S. H.; Yang, Q.-F.; Yi, X.; Shen, B.; Wang, H.; Vahala, K. Bridging Ultrahigh-Q Devices and Photonic Circuits. *Nat. Photonics* **2018**, *12*, 297−302.
(41) Gökbulut, B.; Yartasi, E.; Sunar, E.; Kalaoglu-Altan, O. I.; Gevrek, T. N.; Sanyal, A.; Inci, M. N. Humidity Induced Inhibition and Enhancement of Spontaneous Emission of Dye molecules in a Single PEG Nanofiber. *Opt. Mater. Express* **2018**, *8*, 568−580.

DOI: 10.1021/acs.jpcc.9b05289
J. Phys. Chem. C 2019, 123, 19862−19870